Atmos. Chem. Phys., 21, 7099–7112, 2021
https://doi.org/10.5194/acp-21-7099-2021

Atmospheric Chemistry and Physics
Open Access
EGU

Increased primary and secondary H_2SO_4 showing the opposing roles in secondary organic aerosol formation from ethyl methacrylate ozonolysis

Peng Zhang[1,3,★], **Tianzeng Chen**[1,3,★], **Jun Liu**[1,3], **Guangyan Xu**[1,3], **Qingxin Ma**[1,2,3], **Biwu Chu**[1,2,3], **Wanqi Sun**[4], and **Hong He**[1,2,3]

[1]State Key Joint Laboratory of Environment Simulation and Pollution Control, Research Center for Eco-Environmental Sciences, Chinese Academy of Sciences, Beijing 100085, China
[2]Center for Excellence in Regional Atmospheric Environment, Institute of Urban Environment, Chinese Academy of Sciences, Xiamen 361021, China
[3]University of Chinese Academy of Sciences, Beijing 100049, China
[4]CMA Meteorological Observation Centre, Beijing 100081, China
★These authors contributed equally to this work.

Correspondence: Qingxin Ma (qxma@rcees.ac.cn) and Biwu Chu (bwchu@rcees.ac.cn)

Received: 3 September 2020 – Discussion started: 18 September 2020
Revised: 22 February 2021 – Accepted: 30 March 2021 – Published: 10 May 2021

Abstract. Stressed plants and polymer production can emit many unsaturated volatile organic esters (UVOEs). However, secondary organic aerosol (SOA) formation of UVOEs remains unclear, especially under complex ambient conditions. In this study, we mainly investigated ethyl methacrylate (EM) ozonolysis. Results showed that a substantial increase in secondary H_2SO_4 particles promoted SOA formation with increasing SO_2. An important reason was that the homogeneous nucleation of more H_2SO_4 at high SO_2 level provided greater surface area and volume for SOA condensation. However, increased primary H_2SO_4 with seed acidity enhanced EM uptake but reduced SOA formation. This was ascribed to the fact that the ozonolysis of more adsorbed EM was hampered with the formation of surface H_2SO_4 at higher particle acidity. Moreover, the increase in secondary H_2SO_4 particle via homogeneous nucleation favored to the oligomerization of oxidation products, whereas the increasing of primary H_2SO_4 with acidity in the presence of seed tended to promote the functionalization conversion products. This study indicated that the role of increased H_2SO_4 to EM-derived SOA may not be the same under different ambient conditions, which helps to advance our understanding of the complicated roles of H_2SO_4 in the formation of EM-derived SOA.

1 Introduction

Unsaturated volatile organic esters (UVOEs) are oxygenated volatile organic compounds (OVOCs) with many large-scale commercial uses. They are not only used as potential replacements of traditional solvents and additive in diesel fuels but also are widely used in the production of polymers and resins (Colomer et al., 2013; Taccone et al., 2016; Teruel et al., 2016; Wang et al., 2010). Thus, the production, processing, storage, and disposal of industrial products all contribute to UVOE emissions. In addition, emissions of green leaf volatiles (GLVs), a class of wound-induced OVOCs, also contribute to UVOEs in the atmosphere (Arey et al., 1991; Blanco et al., 2014; Hamilton et al., 2009; Konig et al., 1995). Once emitted into the atmosphere, these UVOEs quickly undergo complex chemical reactions with OH radicals and ozone in sunlight (Bernard et al., 2010; Blanco et al., 2010; Sun et al., 2015), NO_3 radicals during nighttime (Salgado et al., 2011; Wang et al., 2010), and Cl atoms in certain environments (Blanco et al., 2010; Rivela et al., 2018). OH-initiated oxidation of GLVs, including *cis*-3-hexenyl acetate (CHA) to secondary organic aerosol (SOA), is estimated to contribute 1–5 $Tg\,C\,yr^{-1}$, with up to a third of that from isoprene (Hamilton et al., 2009). In addition, CHA-derived SOA

is a more efficient absorber (between 190 and 900 nm) than other OVOCs (such as *cis*-3-hexenol) due to the high proportion of carbonyl-containing species (Harvey et al., 2016). Thus, UVOEs can be considered as a class of potential SOA precursors. Further investigations on UVOE-derived SOA under complex ambient conditions will help to better understand their contribution to ambient aerosol.

Recent studies ascertained that the presence of SO_2 and sulfate seed particles all have a significant impact on the yield, composition, and formation mechanism of SOA (Han et al., 2016; Kristensen et al., 2014; Wong et al., 2015; Zhang et al., 2019). For example, an increase in SO_2 can enhance SOA production due to the formation of more sulfates and the enhanced acid-catalysis role during the atmospheric oxidation of various VOCs (Chu et al., 2016; Lin et al., 2013; Zhao et al., 2018). In the presence of alone seed particles, however, increased particle acidity will not always enhance SOA formation and may have a negligible effect on the SOA formation (Han et al., 2016; Kristensen et al., 2014; Riva et al., 2016; Surratt et al., 2010; Wong et al., 2015; Zhang et al., 2019). Furthermore, it is worth noting that several studies have indicated that an increase in SO_2 can promote the average oxidation state (OS_c) of SOA due to organosulfate formation (Liu et al., 2019a; Shu et al., 2018; Zhang et al., 2019). Whereas other studies have suggested that an increase in SO_2 can have a suppression effect on SOA OS_c (Friedman et al., 2016). Similarly, the effect of increased aerosol acidity on SOA OS_c depends on the contribution of functionalization and oligomerization reactions to SOA composition as increased aerosol acidity can promote these reactions (Shu et al., 2018). This implies that the roles of increased sulfate particles and particle acidity in SOA production and composition are very complicated and need to be further studied.

Methacrylate was one of the main effluents in the class of UVOEs. Just in China, the net import of methacrylate has up to about 930 000 t in 2019. It was worth noting that ethyl methacrylate, one of methacrylate, has been widely detected in ambient air due to the wide variety of sources and high volatility (Pankow et al., 2003). Moreover, some exposure measurement studies indicated that the concentration of ethyl methacrylate was up to 31–108 $\mu g\,m^{-3}$ in the salons working air, which was notably higher than other methacrylate (Henriks-Eckerman and Korva, 2012). Thus, we used ethyl methacrylate (EM) as an UVOE proxy to investigate the effects of different SO_2 levels and seed particle acidity on the formation and evolution of EM-derived SOA in this work. This work will help to better understand the formation of EM-derived SOA under complex conditions.

2 Materials and methods

Multiple EM ozonolysis experiments were conducted in a 30 m^3 cuboid Teflon smog chamber ($L \times W \times H = 3.0\,m \times 2.5\,m \times 4.0\,m$) under 298 K temperature and atmospheric pressure. Experimental conditions are summarized in Table S1 in the Supplement. The chamber operation, analytical techniques, and experimental procedures are described in detail elsewhere (T. Chen et al., 2019). Only a brief description on the specific procedures relevant to this work is presented here.

Prior to each experiment, the chamber was first inflated using purified and dry zero air with a flow rate of 120 $L\,min^{-1}$ for 10 min; subsequently air pump began to run for 5 min. The stainless-steel fan installed at the bottom of chamber was kept to run during the whole cleaning process. Prior to each experiment, Teflon chamber was repeatedly and circularly cleaned by purified and dry zero air using the method above for about 24 h until almost no NO_x could be detected or the particle number concentration was $< 30\,cm^{-3}$. The cleaning procedure of chamber was consistent with that described in our previous studies (T. Z. Chen et al., 2019; Liu et al., 2019a). The O_3 (generated by passing 4 $L\,min^{-1}$ dry zero air over two UV photochemical tubes (40 cm length and 4 cm inner diameter)), SO_2 (520 ppm in N_2, Beijing Huayuan, China), and CO (0.05 % in N_2, Beijing Huayuan, China) were added into the chamber in sequence. EM was first added into a stainless-steel tee at 80 °C and subsequently flushed into the chamber by zero gas with the flow rate of 20 $L\,min^{-1}$. We applied CO to decrease the effect of OH radical reaction via scavenging of OH radicals. The EM (98 % purity, Sigma-Aldrich, USA) was added to the chamber by injection of a known volume into a heated three-way tube (80 °C) and flushed into the chamber by dry zero air. A stainless-steel fan is used to ensure homogeneous mixing of reactants.

To minimize losses in the sampling line, various monitoring instruments surrounded and are next to the smog chamber. The length of sampling pipes of various monitoring instruments ranged from 0.5–1.0 m. A scanning mobility particle sizer (SMPS, TSI, Inc.), consisting of differential mobility analyzer (DMA; model 3082), condensation particle counter (CPC; model 1720), and Po210 bipolar neutralizer, was applied to measure number size distribution. Total particle number and mass concentrations were calculated assuming a uniform density for aerosol particles of 1.4 $g\,cm^{-3}$ (Liu et al., 2019b; T. Chen et al., 2019). The sheath flow and aerosol flow in the SMPS were set to 3.0 and 0.3 $L\,min^{-1}$, respectively. The SMPS results were further corrected via the wall loss rate of $(NH_4)_2SO_4$ particles, and the correction magnitude is about 10 % in a 5 h reaction (Fig. S1 in the Supplement). The desorption or off-gassing of organic gaseous products and NH_3 from chamber wall could be absorbed by seed particles to some extent during introducing seed particles. However, the influence of these particulate species to newly produced secondary particles could be ignorable based on the comparison of their concentrations (Fig. S2).

Based on the different characterized fragments, both mass concentration and evolution of the different chemical compositions of aerosol particles were simultaneously measured online using high-resolution time-of-flight aerosol mass

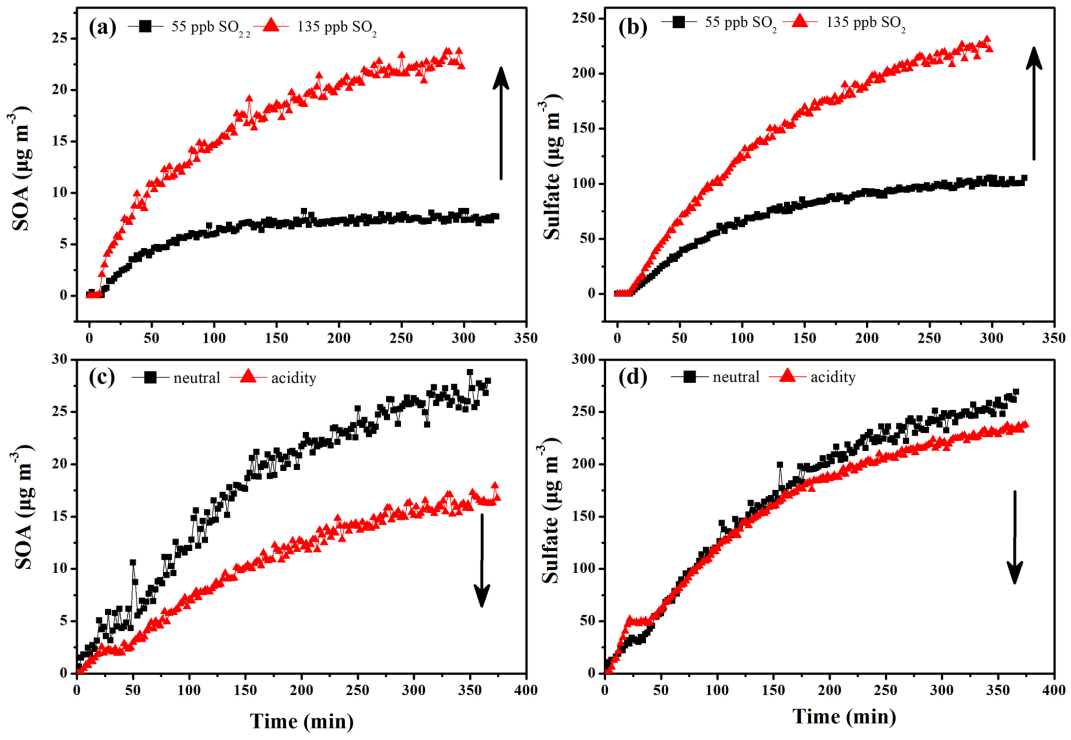

Figure 1. Time-dependent growth curves of SOA **(a)** and sulfate **(b)** under different initial concentrations of SO_2 in absence of seed particles; SOA **(c)** and sulfate **(d)** after subtracting seeds in presence of neutral and acidic seed particles.

spectrometric analysis (HR-ToF-AMS; Aerodyne Research Inc., USA). The AMS working principles and modes of operation are explained in detail elsewhere. According to standard protocols, the inlet flow rate, ionization efficiency (IE), and particle sizing were calibrated using size-selected pure ammonium nitrate (AN) particles (Drewnick et al., 2005). The HR-ToF-AMS analysis toolkit SQUIRREL 1.57I/PIKA v1.16I in Igor Pro v6.37 was employed to process and analyze the experimental data obtained by the HR-ToF-AMS. To reduce the sampling errors resulting from calibrating HR-ToF-AMS before each experiment, the HR-ToF-AMS results were further corrected using mass concentration derived from the SMPS as per Gordon et al. (2014). A series of gas analyzers from Thermo Scientific (USA) were used to monitor the evolution of SO_2 (model 43i), CO (model 48i), and O_3 (model 49i) concentrations as a function of reaction time. Some recent studies indicated that higher CO levels were found to significantly change the chemical composition of SOA relative to low CO level (Zhang et al., 2020; McFiggans et al., 2019). In this work, about 36–38 ppm CO was added in the chamber to exclude OH radical influence during each experiment. Moreover, to make sure results reliable and rule out potential artifacts including the adding sequence of CO, O_3, and SO_2 during experimental preparation and the injection process of EM, parallel experiments (twice experiments at the same experimental conditions) under selected experimental conditions (135 ppb SO_2 and in the presence of AS seeds, respectively) were conducted (Figs. S3 and S4).

3 Results and discussion

3.1 Overview of EM-derived SOA formation with and without seed particles

We first investigated the ozonolysis of alone EM. As shown in Fig. S5, the ozonolysis of alone EM could not produce SOA in the absence of seed and SO_2. Similarly, the increased particle acidity did not promote SOA formation during the ozonolysis of alone EM in the absence of SO_2 (Figs. S6 and S7). Thus, this study mainly focused on EM ozonolysis in the presence of SO_2. Secondary particle formation from EM ozonolysis with different SO_2 levels was first investigated in the absence of seed particles. As shown in Fig. 1, SOA and sulfate were significantly produced once EM was introduced into the reaction chamber. Moreover, both SOA and sulfate formation were markedly enhanced with the increase in initial SO_2 concentration (Fig. 1a and b). This indicated that EM-derived SOA formation was closely related to sulfate formation compared with that the ozonolysis of alone EM. Subsequently, EM ozonolysis with the same level of SO_2 (132–138 ppb) was also conducted in the presence of seed particles with different acidity (neutral and acidic). Two different solutions, including AS (0.02 mol L^{-1})

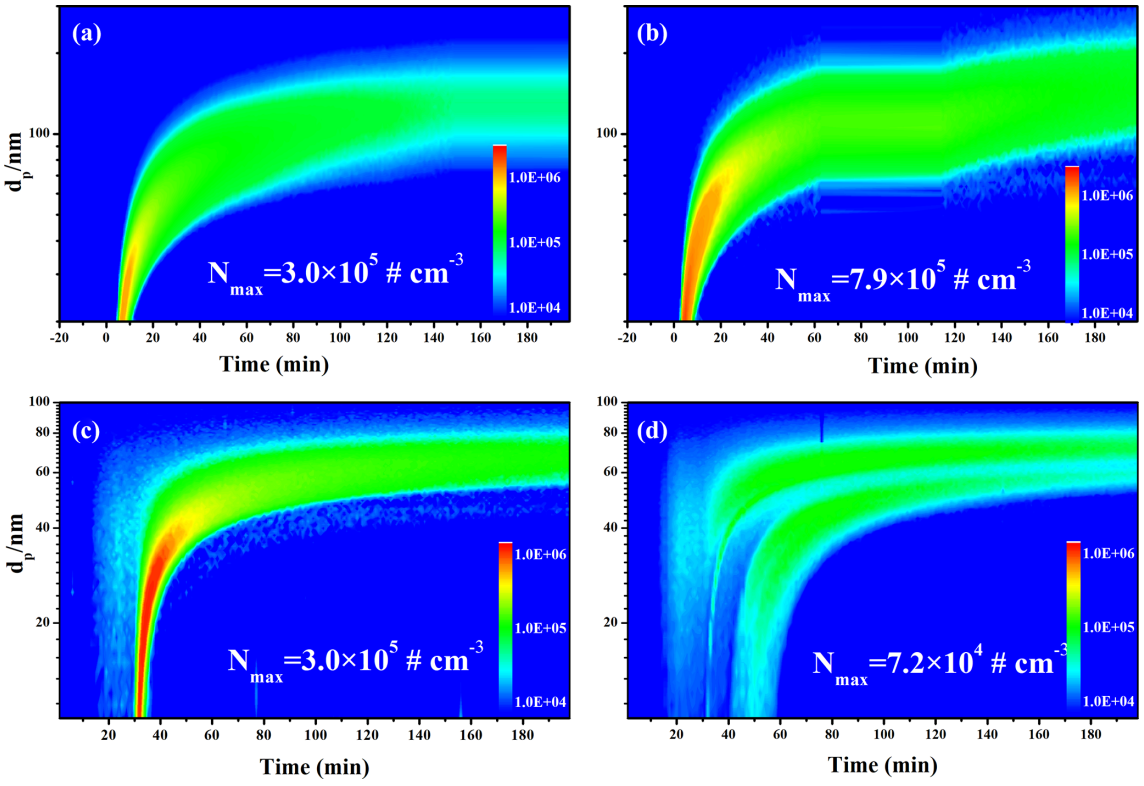

Figure 2. Size distribution of secondary aerosol as a function of time at 55 ppb SO_2 **(a)** and 135 ppb SO_2 **(b)** and under AS seed particle **(c)** and acidic AAS seed particle **(d)**.

and AS + H_2SO_4 (0.02 + 0.04 mol L^{-1}), were nebulized into the chamber, respectively, to provide the corresponding seed aerosol for acidity experiments. The initial seed concentrations can be found in Table S1. Interestingly, with the increase of seed acidity, the maximum mass concentrations of SOA and sulfate decreased from 19.1 to 12.9 µg m^{-3} (Fig. 1c) and 192.6 to 169.7 µg m^{-3} (Fig. 1d), respectively. This indicated that increased particle acidity reduced secondary particle formation in the presence of SO_2, which was inconsistent with the enhancement effect of particle acidity via acid catalysis on SOA formation during alkene photooxidation (such as isoprene, isoprene epoxydiols, and glyoxal) (Kristensen et al., 2014; Lin et al., 2012; Riva et al., 2016; Wong et al., 2015). In order to evaluate whether the effect is atmospherically relevant, these experiments of seed particle role were also conducted at higher RH (45 %–50 % RH). As shown in Fig. S8, it could be found that increased particle acidity also suppressed the formation of SOA and sulfate at higher RH. Thus, these results imply that the increase of primary H_2SO_4 proportion with particle acidity in seed particles and the increase of secondary H_2SO_4 particles with SO_2 concentration exhibited the opposite role in EM-derived SOA formation. In addition, the change in RH was found to have an impact on the formation of EM-derived SOA and sulfate, consistent with our recent studies (Zhang et al., 2019, 2020). SOA concentration at 45 % RH was reduced by a factor of 2 relative to that at 10 % RH in this work (Fig. S9). The changes in both sulfate and SOA concentration were attributed to the competitive reaction between SO_2 and H_2O toward stable Criegee intermediates (sCIs). The suppression of H_2SO_4 concentration was attributed to the rapid consumption of sCI by water and water dimer at high RH (42 %). The suppression of SOA mass loading should be ascribed to the formation of volatile organic peroxides at high RH.

As shown in Fig. 2, the size distributions of secondary particles under different experimental conditions were also compared. The detected maximum particle concentration (790 000 particle cm^{-3}) under 135 ppb SO_2 was higher than that observed under 55 ppb SO_2 (300 000 particle cm^{-3}) in the absence of seed particles (Fig. 2a and b). Recent studies suggested that the reaction between SO_2 and sCI dominated the formation of H_2SO_4 particles and was enhanced with increased SO_2 concentration. An important reason for this is that the rapid homogeneous nucleation of H_2SO_4 not only can provide greater surface area and volume for the condensation of low-volatile products but also reduce the fraction of these semi-volatile species lost to the wall (Chu et al., 2016; Liu et al., 2017; P. Zhang et al., 2019; X. Zhang et al., 2014). The median size distribution of sulfate and surface concentration of fine particles at high SO_2 level supported the conclusion above (Figs. S10 and S11). In the presence of seed particles, we used similar average concentra-

tion ($\sim$ 25 000–30 000 particles cm^{-3}) under different acidities to reduce the disturbance of seed particle concentration (Fig. 2c and d). The mean size and surface concentration of acidified AS (AAS) was higher than AS (Fig. S11B). Results showed $\sim$ 300 000 newly produced particles cm^{-3} for neutral AS seeds (Fig. 2c) and $\sim$ 74 000 newly produced particles cm^{-3} for acidified AS seeds (Fig. 2d), respectively. The reduction of new particle formation (NPF) in the presence of acidic particles most likely results from that acidic seed particles with high mean size, and surface concentration promoted the condensation of gaseous nucleation species onto seed surface. However, this could not explain why both SOA and sulfate were all suppressed with the increase in particle acidity. Thus, one reasonable explanation is that acidic seed particles also enhanced EM uptake on the particle surface as well as promoting the condensation of nucleation species. As a result, the heterogeneous formation of fresher H_2SO_4 on the surface of seed particles subsequently reduced SOA formation by hampering the ozonolysis of absorbed EM. To further support this speculation, we first investigated the EM uptake on the surface of AS solutions with different acidity using a gas mass spectrometer (QMS, GAM 200, Bremen, Germany). As shown in Fig. S12, the increase in H_2SO_4 concentration indeed promoted the uptake of EM on seed particle with the increase of acidity. To further verify whether the presence of SO_2 could hamper the ozonolysis of adsorbed EM due to surface H_2SO_4 formation, we checked and compared the degradation of absorbed EM during its ozonolysis in the absence and presence of SO_2 using the in situ attenuated total internal reflection infrared (ATR-IR) spectra. As shown in Fig. S13, it could be found that EM consumption in the presence of SO_2 was slower than that in the absence of SO_2. This indicated that higher particle acidity indeed promoted EM uptake on the particle surface, and the presence of SO_2 resulted in the residual of more adsorbed EM on particle surface.

In addition, as shown in Figs. S5 and S6, the negligible change of SOA with acidity in the absence of SO_2 also supported the fact that the reducing effect of increasing particle acidity on secondary particle formation was closely related to the formation of H_2SO_4 particles in the presence of SO_2. And some recent studies proved that the presence of inorganic acids HCl may also be an effective scavenger of sCI, further suppressing the formation of low-volatility oligomers (SOA composition) (Zhao et al., 2015). The reaction between sCI and HNO_3 or HCl in particularly was likely to be an important sink of sCI in polluted urban areas under dry conditions (Foreman et al., 2016). Thus, we speculated that the surface secondary reactions between sCI and H_2SO_4 under acidity condition may also suppress the formation of low-volatility oligomers via affecting the sCI lifetime like HCl or HNO_3. Taken together, these results imply that the SOA formation under different SO_2 levels and different particle acidities may be closely related to the homogeneous or heterogeneous formation of H_2SO_4.

3.2 Chemical interpretation and elemental analysis of SOA

Recent studies have suggested that a higher proportion of H_2SO_4 in aerosol can result in greater formation of oligomers and high-oxygenated organic aerosol via acceleration of the acid-catalysis process (Iinuma et al., 2004; Kristensen et al., 2014; Liu et al., 2019a; Rodigast et al., 2017; Shu et al., 2018; Zhang et al., 2019). In order to make clear whether the homogeneous or heterogeneous formation of H_2SO_4 could also affect SOA composition, we further analyze SOA composition and evolution based on positive matrix factorization (PMF) solution and Van Krevelen diagrams (Ulbrich et al., 2009; Zhang et al., 2005). The methodology of PMF analysis can be found in the Supplement (Figs. S14 and S15). The time series and mass spectra of each factor after PMF analysis were applied to characterize the factor constitution and chemical conversion among factors (Ulbrich et al., 2009; Zhang et al., 2005).

Positive matrix factorization (PMF) solution

In the absence of seed particles, two factors were identified under different SO_2 concentrations. As shown in Fig. 3a, the 43 ($C_2H_3O^+$) higher signals (tracers for alcohols and aldehydes) and prominent fragmental peaks containing one-oxygen atom (i.e., C_2H_4O, C_2H_5O, C_3H_5O, C_3H_5O, C_3H_7O, C_4HO, and $C_6H_{10}O$) observed in Factor 2 implied that Factor 2 consisted of less-oxygenated organic aerosols. The 44 (CO_2^+) higher signals, tracers for organic acids, and dominant peaks containing multi-oxygen atoms (i.e., $C_3H_8O_3$, $C_3H_9O_3$, and $C_4H_{10}O_3$) observed in Factor 1 implied that Factor 1 consisted of more-oxygenated organic aerosols. From the temporal variations in Fig. 3b, both Factor 1 and 2 continuously increased with reaction progress before 200 min. This implied that both factors were simultaneously produced, and SOA growth should be mainly attributed to the adsorption and condensation of both less-oxidized species and more-oxidized species on particle before 200 min. After 200 min, Factor 1 continuously increased but Factor 2 decreased, suggesting that the chemical conversion of part of less-oxygenated species in Factor 2 to more-oxygenated products in Factor 1 in the latter period of reaction. Moreover, the average elemental compositions of Factor 1 and Factor 2 were estimated to be $C_{2.29}H_3O_{0.53}S_{0.01}$ and $C_{1.38}H_{1.87}O_{0.37}S_{0.027}$, respectively. Higher OS_c of Factor 2 (-0.85) relative to that Factor 1 (-0.81) also supported the conclusion above. This also implied that the acid-catalyzed role could promote the chemical conversion from Factor 2 to Factor 1 when the H_2SO_4 proportion (acidity) in the particle-phase reached a certain concentration (Liu et al., 2019a; Offenberg et al., 2009). The evolution of m/z 43 and m/z 44 organic fragments, representing the characterized fragment of low- and high-oxidized species, further supported the conclusion above (Fig. S16). As shown in Fig. 3c, the maximum pro-

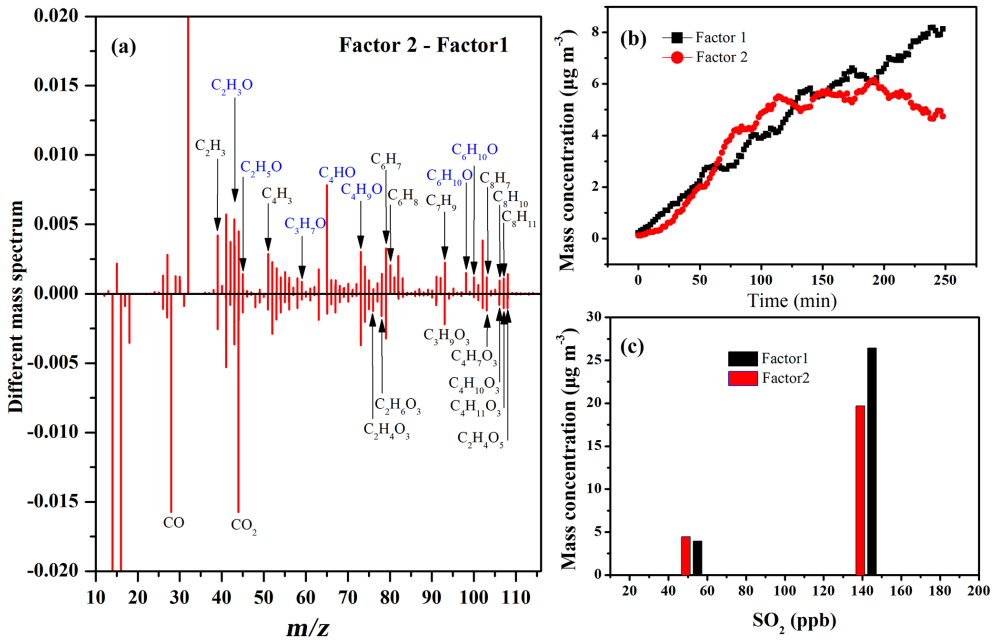

Figure 3. Two-factor solutions for PMF analyses of SOA under different SO_2 concentrations: **(a)** different mass spectra between two factors (Factor 2–Factor 1) at 135 ppb SO_2; **(b)** time series of factor concentrations; **(c)** maximum concentration of two factors at 55 and 135 ppb SO_2.

duction of both Factor 1 and Factor 2 increased with increasing SO_2. One reasonable explanation is that the formation of more H_2SO_4 particles with increasing SO_2 provided a greater surface area and volume for the simultaneous condensation of both less-oxygenated and more-oxygenated organic products (Chu et al., 2016; Liu et al., 2017; Zhang et al., 2019).

In the presence of seed particles, the chemical evolution of SOA components under different acidity conditions was also compared based on PMF analysis. From the temporal variations in Fig. 4a, three factors were identified and almost simultaneously increased. Based on the mass spectra of the three factors (Fig. 4b), the fragments containing less-oxygenated species in Factor 1 (such as typical fragment $C_2H_3O^+$ (*m/z* 43)) were more abundant than in Factor 2. In contrast, the fragments containing more-oxygenated species in Factor 2 (such as typical fragment CO_2^+ (*m/z* 44)) were more abundant than in Factor 1. Thus, Factor 1 and 2 were tentatively assigned to less-oxygenated and more-oxygenated organic aerosols, respectively. This proved that the increase in particle acidity simultaneously promoted the formation of both less- and more-oxygenated species, similar to that in the SO_2 experiments. However, it is worth noting that higher acidity significantly promoted the chemical conversion of less-oxygenated species (Factor 1) to more-oxygenated species (Factor 2) via functionalization based on the comparison between the neutral and acidic seed particles (Fig. 4c). As shown in Fig. 4b, the ion at *m/z* 114 ($C_6H_{10}O_2$) was assigned to precursor-related ions. The highest ion signal fraction (*m/z* 114) in Factor 3 and the similar mass spectrum between EM and Factor 3 in Fig. S13 implied that Factor 3 represented precursor-related species (Fig. 4c).

Based on the comparison of factors between seed experiments and SO_2, it should be noted that Factor 1 and Factor 2 in the seed experiments differed from that in the SO_2 experiment. For SO_2 experiments, acidity appeared to convert Factor 2 to Factor 1 after 200 min, but in seed experiments, the more H_2SO_4 caused the formation of more Factor 2 solutions and fewer Factor 1 solutions. Thus, we concluded that, for the same factor in two types of experiments, the corresponding composition should be different from each other. One possible explanation for this was that the increase in primary and secondary H_2SO_4 particles could also affect SOA composition to some extent, such as via changing the reaction pathway of sCI.

Elemental analysis in Van Krevelen diagrams

The rate at which the H/C ratio changes with the O/C ratio in Van Krevelen diagrams can provide new information about the functional groups formed during oxidation (Chen et al., 2011; Lambe et al., 2012, 2011; Li et al., 2019). As shown in Figs. 5a and 6a, the average (H/C)/(O/C) slopes under different experimental conditions all approached −2. A slope of −2 is due to the formation of carbonyl species (Ng et al., 2011). This is consistent with the acknowledged reaction mechanism of alkene ozonolysis in the presence of SO_2, in which many carbonyl species and H_2SO_4 particles are produced (Newland et al., 2015a, b; Sadezky et al., 2006, 2008). To verify whether increased OS_c was related to par-

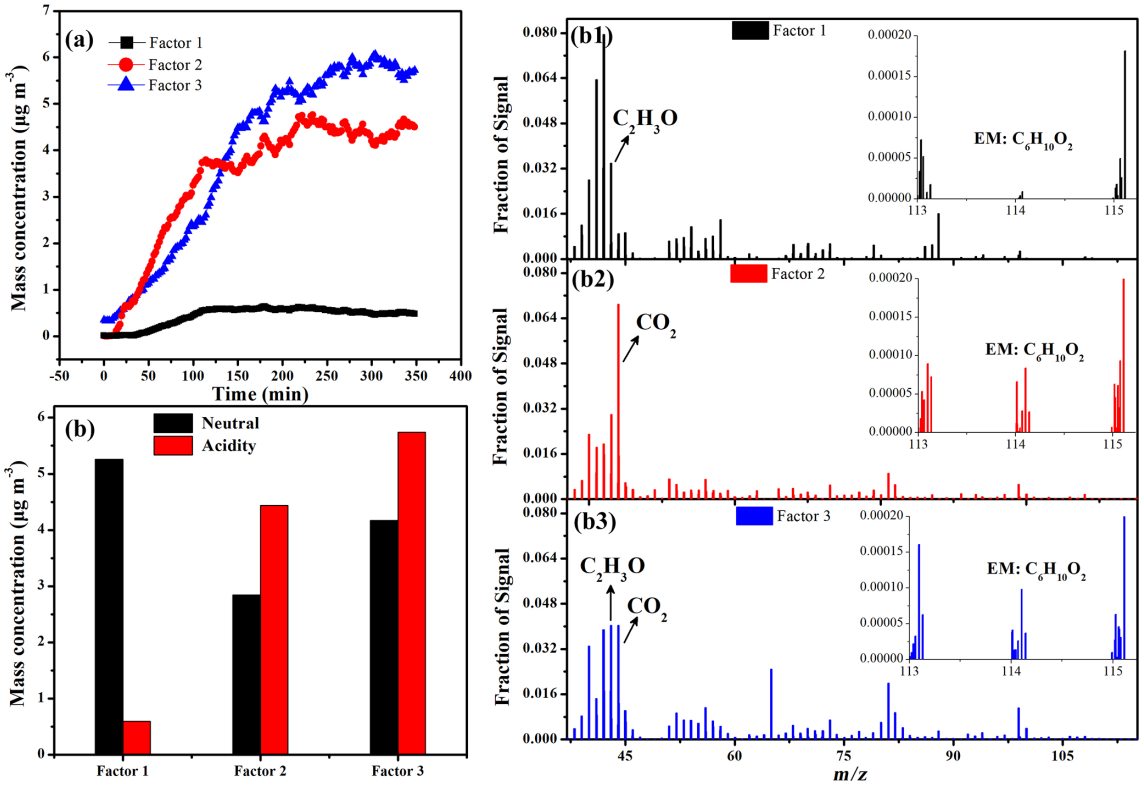

Figure 4. Three-factor solutions for PMF analyses of SOA under different seed particles: **(a)** time series of factor concentrations under acidic AAS; **(b)** mass spectra of three factors; **(c)** comparison of maximum concentration of two factors under neutral AS (black) and acidic AAS (red).

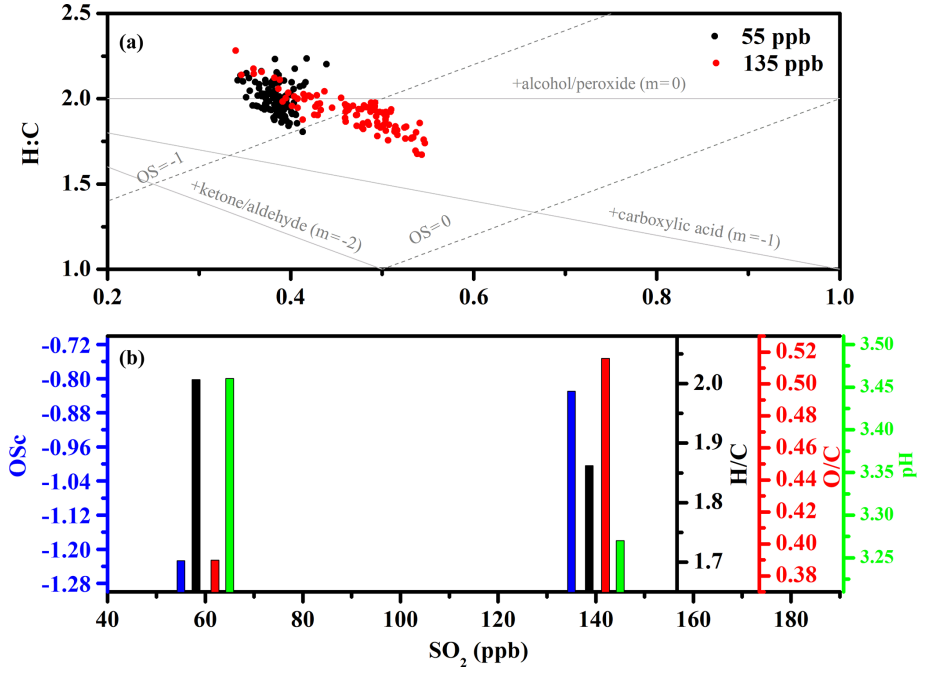

Figure 5. Van Krevelen diagrams of elemental ratios under different initial concentrations of SO_2 **(a)**; change in H/C ratio (black), O/C ratio (red), OS_c (blue), and particle pH (green) as a function of initial SO_2 concentration **(b)**.

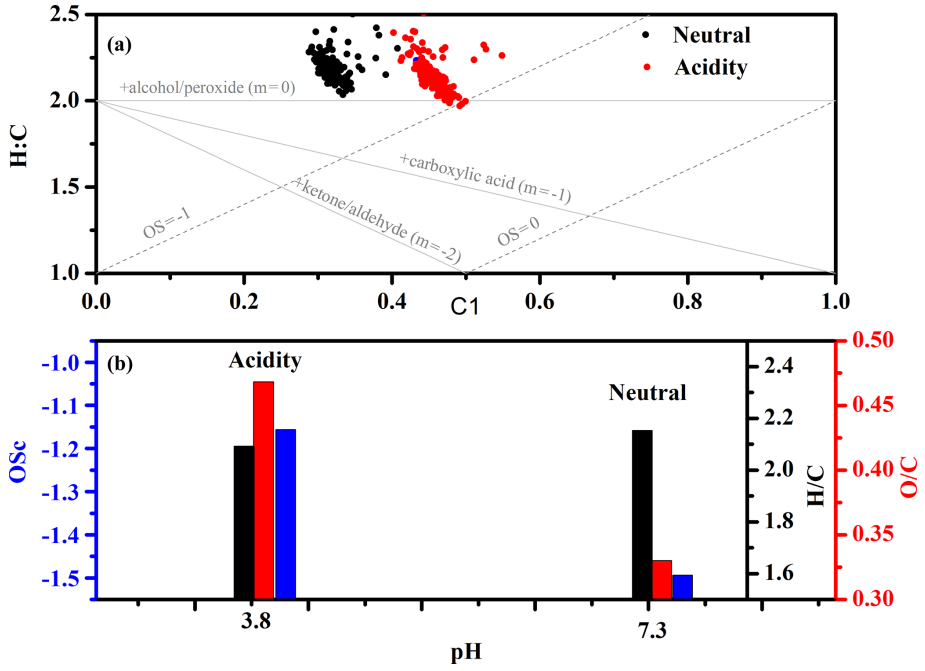

Figure 6. Van Krevelen diagrams of elemental ratios under different seed particle acidity **(a)**; change in H/C ratio (black), O/C ratio (red), and OS_c (blue) with particle acidity **(b)**.

ticle pH, particle pH was estimated using the E-AIM model (Model II: $H^+ - NH_4^+ - SO_4^{2-} - NO_3^- - H_2O$) when secondary particle formation peaked under different SO_2 concentrations (Hennigan et al., 2015; Peng et al., 2019). Since no organics are considered in Model II, there was an inherent assumption here that the acidity and the water uptake was dominated by the inorganic ions. From Fig. 5b, the acidity for nucleated H_2SO_4 particles (pH) under different SO_2 concentration has been estimated to be 3.27 and 3.46, respectively. The acidities for AS and AAS (pH) have been estimated to 7.3 and 4.1, respectively. The averaged oxidation state (OS_c) of SOA increased with decreasing particulate pH in the absence of seeds. A similar trend was also observed in the presence of seed particles (Fig. 6b). This indicated that increased OS_c was closely related to increased particles acidity either in the presence or absence of seed particles. These results also indicated that both functionalization and oligomerization associated with carbonyls groups dominate the formation of EM-derived SOA. Moreover, it is worth noting that O/C increased when H/C decreased with increased particle acidity in the absence of seed particles. In contrast, the O/C ratio increased, but the H/C ratio basically remained stable with increased particle acidity in the presence of seed particles. These results implied that increased particle acidity tended to promote the formation of more highly oxidized products via oligomerization in the absence of seed particles and tended to promote the formation of more highly oxidized products via functionalization in the presence of seed particles (Darer et al., 2011; Shu et al., 2018; Zhang et al., 2019). However, the promoting contribution of SOA functionalization conversion of total SOA could be ignored compared with the reducing effect of acidic particles. Some studies showed that increased OS_c was closely related to the formation of organosulfate (Liu et al., 2019a; Shu et al., 2018; Zhang et al., 2019). To verify the organosulfate formation, the sulfate fragments along with S/C ratio between AS and AAS experiments were also compared. As shown in Fig. S17, the similar S/C ratio and sulfate fragments distribution between neutral and acidic seed experiments excluded the contribution of organosulfate formation to increased OS_c (Y. Chen et al., 2019).

Taken together, in the absence of seed particles, the homogeneous formation of more H_2SO_4 particles not only promoted the quick condensation of less- and more-oxygenated products and subsequent SOA formation via providing a greater surface area and volume but also enhanced the oligomerization process (Fig. 7). In the presence of seed particles, the presence of more primary H_2SO_4 in seed particle enhanced EM uptake and functionalization process but reduced SOA production due to the formation of surface H_2SO_4. This further indicated that the increase in primary and secondary H_2SO_4 particles could significantly affect SOA formation and composition.

3.3 Reaction mechanism of EM ozonolysis

In order to make clear the formation mechanism of EM-derived SOA, the evolutions of some molecular ion peaks have been checked in detail. As shown in Fig. S18, the in-

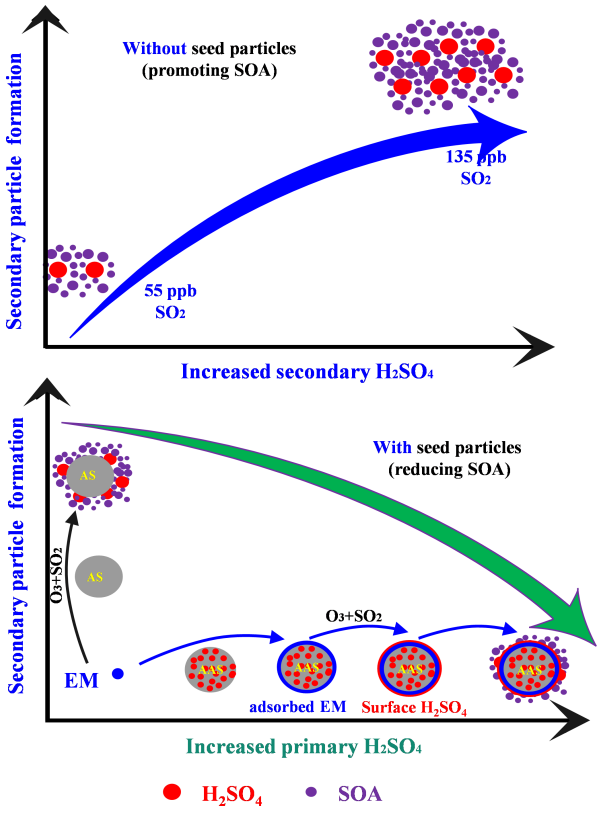

Figure 7. Proposed the role of H_2SO_4 formation on EM-derived SOA.

crease of their mass concentrations with reaction time indicated that these molecular ions peaks with *m/z* 116, 130, 132, 140, 146, 148, 158, 162, 164, 176, 178, 180, 194, 196, and 212 should be the major ozonolysis products. Based on the previously reported mechanism of alkene ozonolysis, the mechanism of EM ozonolysis is proposed in Scheme S1 (Jain et al., 2014; Vereecken and Francisco, 2012). Briefly, oxidation of EM is initiated by addition of ozone across the double bound resulting in a primary ozonide. The primary ozonide will produce two products (formaldehyde and ketone ester) and two sCIs (sCI-1 and sCI-2). Based on the initial carbonyl and sCI products (Scheme S1), it could be found that the saturated ketone ester could not be further oxidized by O_3 and formaldehyde was the terminate products of sCI-2 reaction. Thus, these major oxidation products observed in Fig. S18 should come from the further reaction of sCI-1. The mechanism of EM ozonolysis was proposed based on previous studies (Bianchi et al., 2019; Jokinen et al., 2014; Newland et al., 2018). Some highly oxidized multifunctional compounds could be produced via the H-shift process including 1,7- and 1,8-H shift (Kurten et al., 2015; Mackenzie-Rae et al., 2018). Thus, we concluded that the H-shift followed by autoxidation could be proposed to be a formation pathway of highly oxidized multifunctional compounds.

Proposed reaction mechanism of sCI-1 was also shown in Scheme 1. These sCI-1 could first convert to alkoxy radical (III) by losing OH group and O_2 addition. Then alkoxy radical with an additional oxygen atom not only could further react with RO_2 to form alcohols (V) but also could react with HO_2 to form hydroperoxide product (IV). Moreover, the intramolecular H-shift reaction may also compete with its bimolecular reaction with HO_2 and other RO_2 radicals due to relatively weak C–H bonds in the molecule (Crounse et al., 2013; Jokinen et al., 2014; Shu et al., 2018). Similarly, newly produced alkoxy radical will continually and repeatedly react with HO_2 and RO_2 and undergo its intramolecular H-shift to form the higher oxidized alcohols, carbonyls, and hydroperoxide product. The formation of these higher oxidized alcohols, carbonyls, and hydroperoxide product might help to explain or give insight into the increased oxidation state (OS_c) of the aerosol.

4 Conclusions

Some exposure measurement studies indicated that the concentration of ethyl methacrylate was notably higher than other methacrylate in the salons working air. The frequent exposure of methacrylate for a long time can trigger asthma or allergic contact dermatitis. Thus, the wide variety of sources and high volatility and toxicity make EM a potential important source of environmental concern in the atmosphere. In China, O_3 pollution is gradually becoming a serious environmental problem with the decrease in PM2.5 concentration in recent years. sCI, as a key reactive intermediate in alkene ozonolysis, has been frequently reported to exhibit high oxidation capability in the conversion of SO_2 and NO_2 to secondary particles (Newland et al., 2018). Thus, investigating the ozonolysis of EM under complex condition helps to evaluate their potential contribution to haze formation.

In this work, we investigated and compared the formation of secondary particles from EM ozonolysis under complex ambient conditions. Results showed that a substantial increase in secondary H_2SO_4 particles promoted SOA formation with increasing SO_2. In contrast, the increase in primary H_2SO_4 proportion with seed acidity enhanced EM uptake but reduced SOA formation. To clarify the underlying causes, we analyzed the size distribution, chemical composition, and evolution of SOA based on PMF solutions and Van Krevelen diagrams. In the absence of seed particles, the substantial increase in secondary H_2SO_4 particles with SO_2 provided greater surface area and volume for further condensation of oxidation products. Moreover, enhanced oligomerization functionalization of carbonyl species with increased particle acidity also contributed to the increase in SOA in the absence of seed particles. However, in the presence of seed particles, the increase of primary H_2SO_4 proportion in seed with acidity enhanced more EM uptake, but the direct heterogeneous formation of H_2SO_4 on the particle surface,

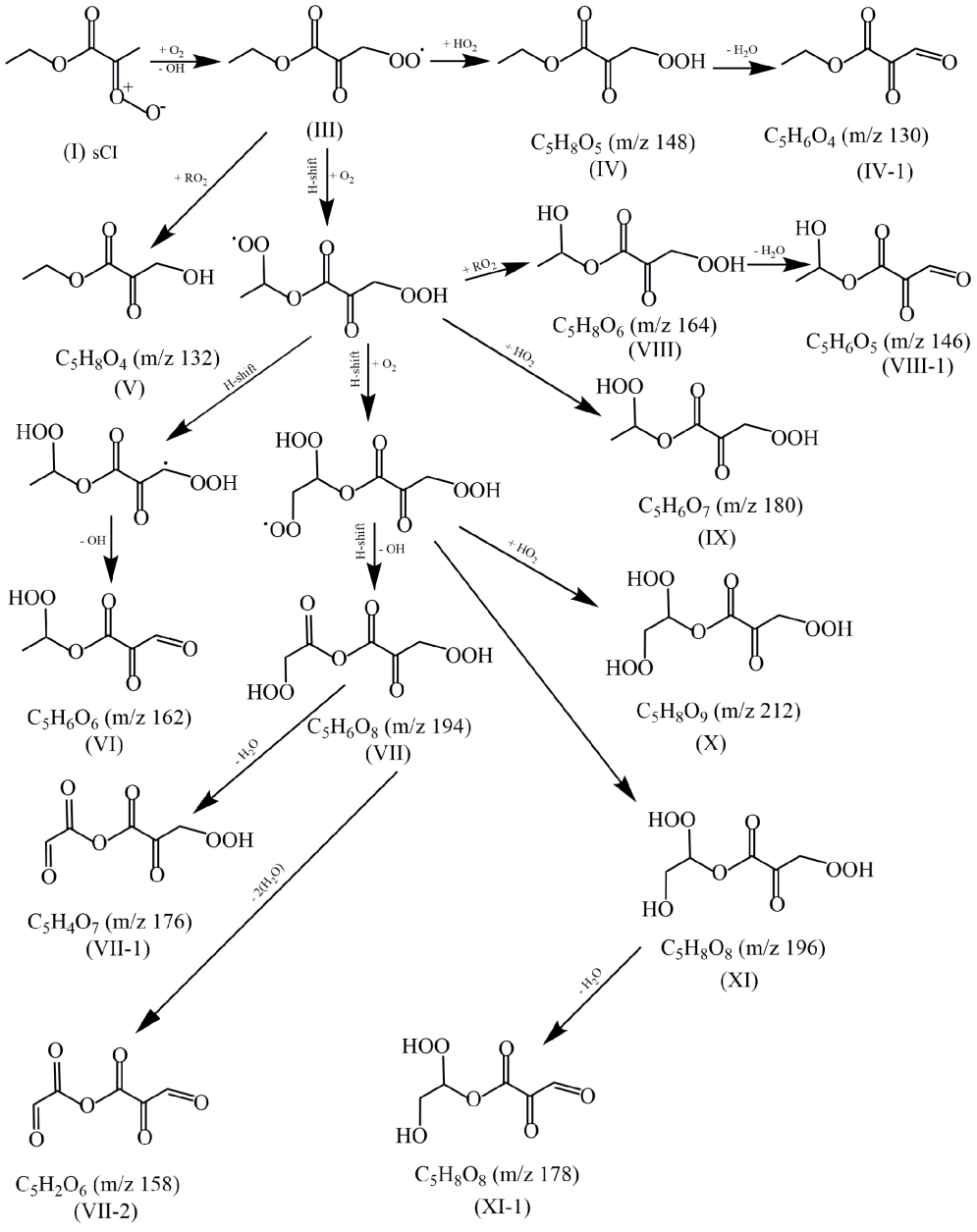

Scheme 1. Proposed mechanism for EM ozonolysis in the presence of AS particles.

differing from the condensation or nucleation of gas-phase H_2SO_4, hampered the continuous heterogeneous ozonolysis of these adsorbed EM. Moreover, even though increased particles acidity also caused chemical conversion of SOA via functionalization, the contribution of the produced functionalized products to SOA could be ignored due to the limited change in overall SOA formation. These results indicated that the increase of primary and secondary H_2SO_4 particle has a different effect on EM-derived SOA formation and its composition.

Taken together, our findings help to further understand the complicated effects of increased H_2SO_4 components on SOA formation and composition during haze pollution. However, more quantitative investigation based on a proton transfer reaction time-of-flight mass spectrometry (PTR-TOFMS) and nitrate ion chemical ionization mass spectrometry (NO_3-CIMS) would be very necessary to accurately evaluate the contribution of H_2SO_4 particles to SOA formation (yield) and composition (molecule structure) in the future study. In addition to EM, many other unsaturated esters such as methyl methacrylate (MA), butyl methacrylate (BMA), and propyl methacrylate (PMA) are also frequently measured in the real atmosphere (Blanco et al., 2014; Ren et al., 2019). Thus, more research is needed to investigate the secondary parti-

cles potential of these unsaturated esters, especially under complex ambient conditions, which will help to further effectively evaluate the potential contribution of their atmospheric oxidation process to secondary particle formation.

Data availability. The experimental data are available upon request to the first or corresponding authors.

Supplement. The supplement related to this article is available online at: https://doi.org/10.5194/acp-21-7099-2021-supplement.

Author contributions. PZ and TC designed and conducted this experiment, TC helped to analyze experimental data. JL, XG, and WS gave assistance in measurements. HH, QM, and BC discussed the data results. PZ wrote the paper with input from all coauthors. All authors contributed to the final paper.

Competing interests. The authors declare that they have no conflict of interest.

Acknowledgements. This work was financially supported by the National Natural Science Foundation of China (21976098, 22006152, 41605100, 41705134, 21876185, 91744205, and 41877304).

Financial support. This work was financially supported by the National Natural Science Foundation of China (21976098, 22006152, 41605100, 41705134, 21876185, 91744205, and 41877304).

Review statement. This paper was edited by Jason Surratt and reviewed by two anonymous referees.

References

Arey, J., Winer, A. M., Atkinson, R., Aschmann, S. M., Long, W. D., and Morrison, C. L.: The Emission of (Z)-3-Hexen-1-Ol, (Z)-3-Hexenylacetate and Other Oxygenated Hydrocarbons from Agricultural Plant-Species, Atmos. Environ. A-Gen., 25, 1063–1075, https://doi.org/10.1016/0960-1686(91)90148-Z, 1991.

Bernard, F., Eyglunent, G., Daele, V., and Mellouki, A.: Kinetics and products of gas-phase reactions of ozone with methyl methacrylate, methyl acrylate, and ethyl acrylate, J. Phys. Chem. A, 114, 8376–8383, https://doi.org/10.1021/jp104451v, 2010.

Bianchi, F., Kurten, T., Riva, M., Mohr, C., Rissanen, M. P., Roldin, P., Berndt, T., Crounse, J. D., Wennberg, P. O., Mentel, T. F., Wildt, J., Junninen, H., Jokinen, T., Kulmala, M., Worsnop, D. R., Thornton, J. A., Donahue, N., Kjaergaard, H. G., and Ehn, M.: Highly Oxygenated Organic Molecules (HOM) from Gas-Phase Autoxidation Involving Peroxy Radicals: A Key Contributor to Atmospheric Aerosol, Chem. Rev., 119, 3472–3509, https://doi.org/10.1021/acs.chemrev.8b00395, 2019.

Blanco, M. B., Bejan, I., Barnes, I., Wiesen, P., and Teruel, M. A.: FTIR product distribution study of the Cl and OH initiated degradation of methyl acrylate at atmospheric pressure, Environ. Sci. Technol., 44, 7031–7036, https://doi.org/10.1021/es101831r, 2010.

Blanco, M. B., Bejan, I., Barnes, I., Wiesen, P., and Teruel, M. A.: Products and mechanism of the reactions of OH radicals and Cl atoms with methyl methacrylate (CH_2=$C(CH_3)C(O)OCH_3$) in the presence of NO_x, Environ. Sci. Technol., 48, 1692–1699, https://doi.org/10.1021/es404771d, 2014.

Chen, Q., Liu, Y., Donahue, N. M., Shilling, J. E., and Martin, S. T.: Particle-phase chemistry of secondary organic material: modeled compared to measured O : C and H : C elemental ratios provide constraints, Environ. Sci. Technol., 45, 4763–4770, https://doi.org/10.1021/es104398s, 2011.

Chen, T., Liu, Y., Ma, Q., Chu, B., Zhang, P., Liu, C., Liu, J., and He, H.: Significant source of secondary aerosol: formation from gasoline evaporative emissions in the presence of SO_2 and NH_3, Atmos. Chem. Phys., 19, 8063–8081, https://doi.org/10.5194/acp-19-8063-2019, 2019.

Chen, T. Z., Liu, Y. C., Liu, C. G., Liu, J., Chu, B. W., and He, H.: Important role of aromatic hydrocarbons in SOA formation from unburned gasoline vapor, Atmos. Environ., 201, 101–109, https://doi.org/10.1016/j.atmosenv.2019.01.001, 2019.

Chen, Y., Xu, L., Humphry, T., Hettiyadura, A. P. S., Ovadnevaite, J., Huang, S., Poulain, L., Schroder, J. C., Campuzano-Jost, P., Jimenez, J. L., Herrmann, H., O'Dowd, C., Stone, E. A., and Ng, N. L.: Response of the Aerodyne Aerosol Mass Spectrometer to Inorganic Sulfates and Organosulfur Compounds: Applications in Field and Laboratory Measurements, Environ. Sci. Technol., 53, 5176–5186, https://doi.org/10.1021/acs.est.9b00884, 2019.

Chu, B., Zhang, X., Liu, Y., He, H., Sun, Y., Jiang, J., Li, J., and Hao, J.: Synergetic formation of secondary inorganic and organic aerosol: effect of SO_2 and NH_3 on particle formation and growth, Atmos. Chem. Phys., 16, 14219–14230, https://doi.org/10.5194/acp-16-14219-2016, 2016.

Colomer, J. P., Blanco, M. B., Penenory, A. B., Barnes, I., Wiesen, P., and Teruel, M. A.: FTIR gas-phase kinetic study on the reactions of OH radicals and Cl atoms with unsaturated esters: Methyl-3,3-dimethyl acrylate, (E)-ethyl tiglate and methyl-3-butenoate, Atmos. Environ., 79, 546–552, https://doi.org/10.1016/j.atmosenv.2013.07.009, 2013.

Crounse, J. D., Nielsen, L. B., Jorgensen, S., Kjaergaard, H. G., and Wennberg, P. O.: Autoxidation of Organic Compounds in the Atmosphere, J. Phys. Chem. Lett., 4, 3513–3520, https://doi.org/10.1021/jz4019207, 2013.

Darer, A. I., Cole-Filipiak, N. C., O'Connor, A. E., and Elrod, M. J.: Formation and stability of atmospherically relevant isoprene-derived organosulfates and organonitrates, Environ. Sci. Technol., 45, 1895–1902, https://doi.org/10.1021/es103797z, 2011.

Drewnick, F., Hings, S. S., DeCarlo, P., Jayne, J. T., Gonin, M., Fuhrer, K., Weimer, S., Jimenez, J. L., Demerjian, K. L., Borrmann, S., and Worsnop, D. R.: A new time-of-flight aerosol mass spectrometer (TOF-AMS) – Instrument description and first field deployment, Aerosol Sci. Tech., 39, 637–658, https://doi.org/10.1080/02786820500182040, 2005.

Foreman, E. S., Kapnas, K. M., and Murray, C.: Reactions between Criegee Intermediates and the Inorganic Acids HCl and HNO_3: Kinetics and Atmospheric Implications, Angew. Chem. Int. Edit., 55, 10419–10422, https://doi.org/10.1002/anie.201604662, 2016.

Friedman, B., Brophy, P., Brune, W. H., and Farmer, D. K.: Anthropogenic Sulfur perturbations on biogenic oxidation: SO_2 additions impact gas-phase oh oxidation products of α- and β-pinene, Environ. Sci. Technol., 50, 1269–1279, https://doi.org/10.1021/acs.est.5b05010, 2016.

Gordon, T. D., Presto, A. A., May, A. A., Nguyen, N. T., Lipsky, E. M., Donahue, N. M., Gutierrez, A., Zhang, M., Maddox, C., Rieger, P., Chattopadhyay, S., Maldonado, H., Maricq, M. M., and Robinson, A. L.: Secondary organic aerosol formation exceeds primary particulate matter emissions for light-duty gasoline vehicles, Atmos. Chem. Phys., 14, 4661–4678, https://doi.org/10.5194/acp-14-4661-2014, 2014.

Hamilton, J. F., Lewis, A. C., Carey, T. J., Wenger, J. C., Borrás i Garcia, E., and Muñoz, A.: Reactive oxidation products promote secondary organic aerosol formation from green leaf volatiles, Atmos. Chem. Phys., 9, 3815–3823, https://doi.org/10.5194/acp-9-3815-2009, 2009.

Han, Y., Stroud, C. A., Liggio, J., and Li, S.-M.: The effect of particle acidity on secondary organic aerosol formation from α-pinene photooxidation under atmospherically relevant conditions, Atmos. Chem. Phys., 16, 13929–13944, https://doi.org/10.5194/acp-16-13929-2016, 2016.

Harvey, R. M., Bateman, A. P., Jain, S., Li, Y. J., Martin, S., and Petrucci, G. A.: Optical Properties of Secondary Organic Aerosol from cis-3-Hexenol and cis-3-Hexenyl Acetate: Effect of Chemical Composition, Humidity, and Phase, Environ. Sci. Technol., 50, 4997–5006, https://doi.org/10.1021/acs.est.6b00625, 2016.

Hennigan, C. J., Izumi, J., Sullivan, A. P., Weber, R. J., and Nenes, A.: A critical evaluation of proxy methods used to estimate the acidity of atmospheric particles, Atmos. Chem. Phys., 15, 2775–2790, https://doi.org/10.5194/acp-15-2775-2015, 2015.

Henriks-Eckerman, M. L. and Korva, M.: Exposure to airborne methacrylates in nail salons, J. Occup. Environ. Hyg., 9, D146–D150, https://doi.org/10.1080/15459624.2012.696023, 2012.

Iinuma, Y., Boge, O., Gnauk, T., and Herrmann, H.: Aerosol-chamber study of the α-pinene/O_3 reaction: influence of particle acidity on aerosol yields and products, Atmos. Environ., 38, 761–773, https://doi.org/10.1016/j.atmosenv.2003.10.015, 2004.

Jain, S., Zahardis, J., and Petrucci, G. A.: Soft ionization chemical analysis of secondary organic aerosol from green leaf volatiles emitted by turf grass, Environ. Sci. Technol., 48, 4835–4843, https://doi.org/10.1021/es405355d, 2014.

Jokinen, T., Sipila, M., Richters, S., Kerminen, V. M., Paasonen, P., Stratmann, F., Worsnop, D., Kulmala, M., Ehn, M., Herrmann, H., and Berndt, T.: Rapid autoxidation forms highly oxidized RO_2 radicals in the atmosphere, Angew. Chem. Int. Edit., 53, 14596–14600, https://doi.org/10.1002/anie.201408566, 2014.

Konig, G., Brunda, M., Puxbaum, H., Hewitt, C. N., Duckham, S. C., and Rudolph, J.: Relative contribution of oxygenated hydrocarbons to the total biogenic voc emissions of selected mid-european agricultural and natural plant-species, Atmos. Environ., 29, 861–874, https://doi.org/10.1016/1352-2310(95)00026-U, 1995.

Kristensen, K., Cui, T., Zhang, H., Gold, A., Glasius, M., and Surratt, J. D.: Dimers in α-pinene secondary organic aerosol: effect of hydroxyl radical, ozone, relative humidity and aerosol acidity, Atmos. Chem. Phys., 14, 4201–4218, https://doi.org/10.5194/acp-14-4201-2014, 2014.

Kurten, T., Rissanen, M. P., Mackeprang, K., Thornton, J. A., Hyttinen, N., Jorgensen, S., Ehn, M., and Kjaergaard, H. G.: Computational study of hydrogen shifts and ring-opening mechanisms in alpha-pinene ozonolysis products, J. Phys. Chem. A, 119, 11366–11375, https://doi.org/10.1021/acs.jpca.5b08948, 2015.

Lambe, A. T., Onasch, T. B., Massoli, P., Croasdale, D. R., Wright, J. P., Ahern, A. T., Williams, L. R., Worsnop, D. R., Brune, W. H., and Davidovits, P.: Laboratory studies of the chemical composition and cloud condensation nuclei (CCN) activity of secondary organic aerosol (SOA) and oxidized primary organic aerosol (OPOA), Atmos. Chem. Phys., 11, 8913–8928, https://doi.org/10.5194/acp-11-8913-2011, 2011.

Lambe, A. T., Onasch, T. B., Croasdale, D. R., Wright, J. P., Martin, A. T., Franklin, J. P., Massoli, P., Kroll, J. H., Canagaratna, M. R., Brune, W. H., Worsnop, D. R., and Davidovits, P.: Transitions from functionalization to fragmentation reactions of laboratory secondary organic aerosol (SOA) generated from the OH oxidation of alkane precursors, Environ. Sci. Technol., 46, 5430–5437, https://doi.org/10.1021/es300274t, 2012.

Li, K., Liggio, J., Lee, P., Han, C., Liu, Q., and Li, S.-M.: Secondary organic aerosol formation from α-pinene, alkanes, and oil-sands-related precursors in a new oxidation flow reactor, Atmos. Chem. Phys., 19, 9715–9731, https://doi.org/10.5194/acp-19-9715-2019, 2019.

Lin, Y. H., Zhang, Z. F., Docherty, K. S., Zhang, H. F., Budisulistiorini, S. H., Rubitschun, C. L., Shaw, S. L., Knipping, E. M., Edgerton, E. S., Kleindienst, T. E., Gold, A., and Surratt, J. D.: Isoprene epoxydiols as precursors to secondary organic aerosol formation: acid-catalyzed reactive uptake studies with authentic compounds, Environ. Sci. Technol., 46, 250–258, https://doi.org/10.1021/es202554c, 2012.

Lin, Y.-H., Knipping, E. M., Edgerton, E. S., Shaw, S. L., and Surratt, J. D.: Investigating the influences of SO_2 and NH_3 levels on isoprene-derived secondary organic aerosol formation using conditional sampling approaches, Atmos. Chem. Phys., 13, 8457–8470, https://doi.org/10.5194/acp-13-8457-2013, 2013.

Liu, C., Chen, T., Liu, Y., Liu, J., He, H., and Zhang, P.: Enhancement of secondary organic aerosol formation and its oxidation state by SO_2 during photooxidation of 2-methoxyphenol, Atmos. Chem. Phys., 19, 2687–2700, https://doi.org/10.5194/acp-19-2687-2019, 2019a.

Liu, C., Liu, Y., Chen, T., Liu, J., and He, H.: Rate constant and secondary organic aerosol formation from the gas-phase reaction of eugenol with hydroxyl radicals, Atmos. Chem. Phys., 19, 2001–2013, https://doi.org/10.5194/acp-19-2001-2019, 2019b.

Liu, S., Jia, L., Xu, Y., Tsona, N. T., Ge, S., and Du, L.: Photooxidation of cyclohexene in the presence of SO_2: SOA yield and chemical composition, Atmos. Chem. Phys., 17, 13329–13343, https://doi.org/10.5194/acp-17-13329-2017, 2017.

Mackenzie-Rae, F. A., Wallis, H. J., Rickard, A. R., Pereira, K. L., Saunders, S. M., Wang, X., and Hamilton, J. F.: Ozonolysis of α-phellandrene – Part 2: Compositional analysis of secondary organic aerosol highlights the role of stabilised

Criegee intermediates, Atmos. Chem. Phys., 18, 4673–4693, https://doi.org/10.5194/acp-18-4673-2018, 2018.

McFiggans, G., Mentel, T. F., Wildt, J., Pullinen, I., Kang, S., Kleist, E., Schmitt, S., Springer, M., Tillmann, R., Wu, C., Zhao, D., Hallquist, M., Faxon, C., Le Breton, M., Hallquist, A. M., Simpson, D., Bergstrom, R., Jenkin, M. E., Ehn, M., Thornton, J. A., Alfarra, M. R., Bannan, T. J., Percival, C. J., Priestley, M., Topping, D., and Kiendler-Scharr, A.: Secondary organic aerosol reduced by mixture of atmospheric vapours, Nature, 565, 587–593, https://doi.org/10.1038/s41586-018-0871-y, 2019.

Newland, M. J., Rickard, A. R., Alam, M. S., Vereecken, L., Munoz, A., Rodenas, M., and Bloss, W. J.: Kinetics of stabilised Criegee intermediates derived from alkene ozonolysis: reactions with SO_2, H_2O and decomposition under boundary layer conditions, Phys. Chem. Chem. Phys., 17, 4076–4088, https://doi.org/10.1039/c4cp04186k, 2015a.

Newland, M. J., Rickard, A. R., Vereecken, L., Muñoz, A., Ródenas, M., and Bloss, W. J.: Atmospheric isoprene ozonolysis: impacts of stabilised Criegee intermediate reactions with SO_2, H_2O and dimethyl sulfide, Atmos. Chem. Phys., 15, 9521–9536, https://doi.org/10.5194/acp-15-9521-2015, 2015b.

Newland, M. J., Rickard, A. R., Sherwen, T., Evans, M. J., Vereecken, L., Muñoz, A., Ródenas, M., and Bloss, W. J.: The atmospheric impacts of monoterpene ozonolysis on global stabilised Criegee intermediate budgets and SO_2 oxidation: experiment, theory and modelling, Atmos. Chem. Phys., 18, 6095–6120, https://doi.org/10.5194/acp-18-6095-2018, 2018.

Ng, N. L., Canagaratna, M. R., Jimenez, J. L., Chhabra, P. S., Seinfeld, J. H., and Worsnop, D. R.: Changes in organic aerosol composition with aging inferred from aerosol mass spectra, Atmos. Chem. Phys., 11, 6465–6474, https://doi.org/10.5194/acp-11-6465-2011, 2011.

Offenberg, J. H., Lewandowski, M., Edney, E. O., Kleindienst, T. E., and Jaoui, M.: Influence of aerosol acidity on the formation of secondary organic aerosol from biogenic precursor hydrocarbons, Environ. Sci. Technol., 43, 7742–7747, https://doi.org/10.1021/es901538e, 2009.

Pankow, J. F., Luo, W. T., Bender, D. A., Isabelle, L. M., Hollingsworth, J. S., Chen, C., Asher, W. E., and Zogorski, J. S.: Concentrations and co-occurrence correlations of 88 volatile organic compounds (VOCs) in the ambient air of 13 semi-rural to urban locations in the United States, Atmos. Environ., 37, 5023–5046, https://doi.org/10.1016/j.atmosenv.2003.08.006, 2003.

Peng, X., Vasilakos, P., Nenes, A., Shi, G., Qian, Y., Shi, X., Xiao, Z., Chen, K., Feng, Y., and Russell, A. G.: Detailed analysis of estimated ph, activity coefficients, and ion concentrations between the three aerosol thermodynamic models, Environ. Sci. Technol., 53, 8903–8913, https://doi.org/10.1021/acs.est.9b00181, 2019.

Ren, Y. G., Cai, M., Daele, V., and Mellouki, A.: Rate coefficients for the reactions of OH radical and ozone with a series of unsaturated esters, Atmos. Environ., 200, 243–253, https://doi.org/10.1016/j.atmosenv.2018.12.017, 2019.

Riva, M., Bell, D. M., Hansen, A. M., Drozd, G. T., Zhang, Z., Gold, A., Imre, D., Surratt, J. D., Glasius, M., and Zelenyuk, A.: Effect of organic coatings, humidity and aerosol acidity on multiphase chemistry of isoprene epoxydiols, Environ. Sci. Technol., 50, 5580–5588, https://doi.org/10.1021/acs.est.5b06050, 2016.

Rivela, C. B., Blanco, M. B., and Teruel, M. A.: Atmospheric degradation of industrial fluorinated acrylates and methacrylates with Cl atoms at atmospheric pressure and 298 K, Atmos. Environ., 178, 206–213, https://doi.org/10.1016/j.atmosenv.2018.01.055, 2018.

Rodigast, M., Mutzel, A., and Herrmann, H.: A quantification method for heat-decomposable methylglyoxal oligomers and its application on 1,3,5-trimethylbenzene SOA, Atmos. Chem. Phys., 17, 3929–3943, https://doi.org/10.5194/acp-17-3929-2017, 2017.

Sadezky, A., Chaimbault, P., Mellouki, A., Römpp, A., Winterhalter, R., Le Bras, G., and Moortgat, G. K.: Formation of secondary organic aerosol and oligomers from the ozonolysis of enol ethers, Atmos. Chem. Phys., 6, 5009–5024, https://doi.org/10.5194/acp-6-5009-2006, 2006.

Sadezky, A., Winterhalter, R., Kanawati, B., Römpp, A., Spengler, B., Mellouki, A., Le Bras, G., Chaimbault, P., and Moortgat, G. K.: Oligomer formation during gas-phase ozonolysis of small alkenes and enol ethers: new evidence for the central role of the Criegee Intermediate as oligomer chain unit, Atmos. Chem. Phys., 8, 2667–2699, https://doi.org/10.5194/acp-8-2667-2008, 2008.

Salgado, M. S., Gallego-Iniesta, M. P., Martin, M. P., Tapia, A., and Cabanas, B.: Night-time atmospheric chemistry of methacrylates, Environ. Sci. Pollut. Res. Int., 18, 940–948, https://doi.org/10.1007/s11356-011-0448-x, 2011.

Shu, Y. J., Ji, J., Xu, Y., Deng, J. G., Huang, H. B., He, M., Leung, D. Y. C., Wu, M. Y., Liu, S. W., Liu, S. L., Liu, G. Y., Xie, R. J., Feng, Q. Y., Zhan, Y. J., Fang, R. M., and Ye, X. G.: Promotional role of Mn doping on catalytic oxidation of VOCs over mesoporous TiO_2 under vacuum ultraviolet (VUV) irradiation, Appl. Catal. B-Environ., 220, 78–87, https://doi.org/10.1016/j.apcatb.2017.08.019, 2018.

Sun, Y., Zhang, Q., Hu, J., Chen, J., and Wang, W.: Theoretical study for OH radical-initiated atmospheric oxidation of ethyl acrylate, Chemosphere, 119, 626–633, https://doi.org/10.1016/j.chemosphere.2014.07.056, 2015.

Surratt, J. D., Chan, A. W., Eddingsaas, N. C., Chan, M., Loza, C. L., Kwan, A. J., Hersey, S. P., Flagan, R. C., Wennberg, P. O., and Seinfeld, J. H.: Reactive intermediates revealed in secondary organic aerosol formation from isoprene, P. Natl. Acad. Sci. USA., 107, 6640–6645, https://doi.org/10.1073/pnas.0911114107, 2010.

Taccone, R. A., Moreno, A., Colmenar, I., Salgado, S., Martin, M. P., and Cabanas, B.: Kinetic study of the OH, NO_3 radicals and Cl atom initiated atmospheric photo-oxidation of Iso-propenyl methyl ether, Atmos. Environ., 127, 80–89, https://doi.org/10.1016/j.atmosenv.2015.12.033, 2016.

Teruel, M. A., Lopez, R. S. P., Barnes, I., and Blanco, M. B.: Night-time atmospheric degradation of a series of butyl methacrylates, Chem. Phys. Lett., 664, 205–212, https://doi.org/10.1016/j.cplett.2016.09.040, 2016.

Ulbrich, I. M., Canagaratna, M. R., Zhang, Q., Worsnop, D. R., and Jimenez, J. L.: Interpretation of organic components from Positive Matrix Factorization of aerosol mass spectrometric data, Atmos. Chem. Phys., 9, 2891–2918, https://doi.org/10.5194/acp-9-2891-2009, 2009.

Vereecken, L. and Francisco, J. S.: Theoretical studies of atmospheric reaction mechanisms in the troposphere, Chem. Soc. Rev., 41, 6259–6293, https://doi.org/10.1039/c2cs35070j, 2012.

Wang, K., Ge, M. F., and Wang, W. G.: Kinetics of the gas-phase reactions of NO_3 radicals with ethyl acrylate, n-butyl acrylate, methyl methacrylate and ethyl methacrylate, Atmos. Environ., 44, 1847–1850, https://doi.org/10.1016/j.atmosenv.2010.02.039, 2010.

Wong, J. P., Lee, A. K., and Abbatt, J. P.: Impacts of sulfate seed acidity and water content on isoprene secondary organic aerosol formation, Environ. Sci. Technol., 49, 13215–13221, https://doi.org/10.1021/acs.est.5b02686, 2015.

Zhang, P., Chen, T., Liu, J., Liu, C., Ma, J., Ma, Q., Chu, B., and He, H.: Impacts of SO_2, Relative humidity, and seed acidity on secondary organic aerosol formation in the ozonolysis of butyl vinyl ether, Environ. Sci. Technol., 53, 8845–8853, https://doi.org/10.1021/acs.est.9b02702, 2019.

Zhang, P., Chen, T., Liu, J., Chu, B., Ma, Q., Ma, J., and He, H.: Impacts of mixed gaseous and particulate pollutants on secondary particle formation during ozonolysis of butyl vinyl ether, Environ. Sci. Technol., 54, 3909–3919, https://doi.org/10.1021/acs.est.9b07650, 2020.

Zhang, Q., Alfarra, M. R., Worsnop, D. R., Allan, J. D., Coe, H., Canagaratna, M. R., and Jimenez, J. L.: Deconvolution and quantification of hydrocarbon-like and oxygenated organic aerosols based on aerosol mass spectrometry, Environ. Sci. Technol., 39, 4938–4952, https://doi.org/10.1021/es048568l, 2005.

Zhang, X., Cappa, C. D., Jathar, S. H., McVay, R. C., Ensberg, J. J., Kleeman, M. J., and Seinfeld, J. H.: Influence of vapor wall loss in laboratory chambers on yields of secondary organic aerosol, P. Natl. Acad. Sci. USA, 111, 5802–5807, https://doi.org/10.1073/pnas.1404727111, 2014.

Zhao, D., Schmitt, S. H., Wang, M., Acir, I.-H., Tillmann, R., Tan, Z., Novelli, A., Fuchs, H., Pullinen, I., Wegener, R., Rohrer, F., Wildt, J., Kiendler-Scharr, A., Wahner, A., and Mentel, T. F.: Effects of NO_x and SO_2 on the secondary organic aerosol formation from photooxidation of α-pinene and limonene, Atmos. Chem. Phys., 18, 1611–1628, https://doi.org/10.5194/acp-18-1611-2018, 2018.

Zhao, Y., Wingen, L. M., Perraud, V., Greaves, J., and Finlayson-Pitts, B. J.: Role of the reaction of stabilized Criegee intermediates with peroxy radicals in particle formation and growth in air, Phys. Chem. Chem. Phys., 17, 12500–12514, https://doi.org/10.1039/c5cp01171j, 2015.